Process for the fabrication of complex three-dimensional microcoils in fused silica

Feng Chen,* Chao Shan, Keyin Liu, Qing Yang, Xiangwei Meng, Shengguan He, Jinhai Si, Feng Yun, and Xun Hou

State Key Laboratory for Manufacturing System Engineering & Key Laboratory of Photonics Technology for Information of Shaanxi Province, School of Electronics & Information Engineering, Xi'an Jiaotong University, Xi'an 710049, China

**Corresponding author: chenfeng@mail.xjtu.edu.cn*

Received June 14, 2013; revised July 4, 2013; accepted July 11, 2013;
posted July 11, 2013 (Doc. ID 192039); published August 1, 2013

The creation of complex three-dimensional (3D) microcoils has attracted significant attention from both scientific and applied research communities. However, it still remains challenging to build 3D microcoils with arbitrary configurations using conventional planar lithographic fabrication methods. This Letter presents a new facile method based on an improved femtosecond laser wet etch technology and metal microsolidifying process for the fabrication of on-chip complex 3D microcoils inside fused silica. The diameter of the microcoils is about 30 μm, and the effective length of the microchannel is about 13 mm. The aspect ratio of the microcoils can be larger than 400:1, and the microchannel exhibiting good uniformity and smoothness also has good flowability for high-viscosity conductive gallium metal. Based on this approach, we fabricated complex microcoils such as U-shaped and O-shaped microcoils that can be easily integrated into a "lab on a chip" platform or microelectric system inside fused-silica substrate.

OCIS codes: (140.3390) Laser materials processing; (220.4000) Microstructure fabrication; (220.4610) Optical fabrication; (220.4241) Nanostructure fabrication.

http://dx.doi.org/10.1364/OL.38.002911

Microcoils, like bones of a body for the microelectromechanical systems (MEMS), have a wide variety of applications. Recently, many efforts have been made focusing on the fabrication of microcoils [1–3]. The mainstream fabrication techniques, which heavily rely on the well-established two-dimensional (2D) planar lithographic approach, have advanced to the degree of miniaturization and precision of the microcoil manufacturing process. However, the application of these 2D flat coils usually results in an inhomogeneous magnetic field, low inductance value, small quality factor, and large volume. As compared to the shortcomings of 2D planar microcoils, true three-dimensional (3D) microcoils have a well-controlled 3D magnetic field, higher sensitivity, and less volume. Complex 3D microcoils, especially, have high integration, efficiency, and microfield control capabilities and can easily integrate with other MEMS devices serving a broader range of applications. Typical examples include sensors and actuators for magnetic field measurement and flaw detection in materials, microinductors for electronic circuits, micropositioners, and microactuators for microsystems [4–7].

The processes to fabricate 3D microcoils include multilayer photolithography and electroplating [8–10], winding a metal wire around a yoke, and creating helical conducting paths on a cylinder [11–14]. However, these methods are too complex and difficult to fabricate for on-chip 3D microcoils. There is an unfulfilled demand for a facile method to fabricate the integratable on-chip 3D microcoils for micrototal analysis systems applications to address the above-mentioned issues [15]. On such demand, femtosecond laser micromachining has become a new tool to fabricate 3D structures inside transparent materials. Recently, there has been much research on flexible nanowiring of metal on nonplanar substrates by femtosecond-laser-induced electroless plating. A series of silver nanowires have been successfully produced for the applications on microheaters [16]. However, the polymer material is not suitable for the integrated "lab on a chip" (LoC) system. Therefore, there is a need for a method of manufacturing microcoils inside fused silica, which serves as an ideal material for LoC applications due to its very high optical transparency, low background fluorescence, chemical inertness, and hydrophilicity [15].

In this Letter, we present a facile method based on femtosecond laser wet etch (FLWE) technology and a metal microsolidifying process to fabricate on-chip complex 3D microcoils with good channel uniformity and smoothness inside fused silica. This work pays more attention to the practical application of the complex 3D microcoil device structures and properties, such as good uniformity, smoothness, and flow ability for high-viscosity conductive gallium metal. Four major improvements, including slower femtosecond laser writing speed, lower laser power, lower hydrofluoric acid (HF) concentration, and longer etch time, have been employed to fabricate the complex 3D microcoils. This complex microcoil fabrication technology is beneficial for developing good integration for magnetic resonance imaging (MRI) and nuclear magnetic resonance (NMR) in the future.

The microcoil manufacturing process is schematically represented in Fig. 1. It includes two steps: production of 3D microchannels, and injection with metal gallium into the channels in the fused silica. In order to produce the 3D helical microchannels, a femtosecond laser beam, which is created by a Ti:sapphire pulsed laser oscillator-amplifier system (wavelength = 800 nm; pulse duration = 50 fs; repetition rate = 1 kHz), is

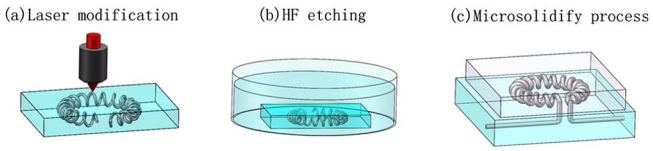

Fig. 1. Schematic diagram of the fabrication process.

focused inside the fused-silica substrate (1.0 mm × 1.0 mm × 1.0 mm) by a microscope objective lens (NA = 0.9, objective magnification is 100, working distance is 2 mm, depth of field is 0.5 μm, Nikon). The channel is written by the laser through translating the 3D stage (the xyz resolution of the stage is 40 nm, the model of the stage is H101A ProScan II Upright Stage made by Prior Scientific) along the pattern path with a speed of 10 μm/s, as shown in Fig. 1(a).

As opposed to linearly polarized laser light, circularly polarized laser light is used in the manufacture of a complex 3D microchannel with a high etching rate. The laser power is adjusted by a computer-controlled attenuator with the temporal modulation of the power compensation. The geometry of the coil, the height, and the pitch circle diameter of the helix can be controlled by a computer. Then, the coil sample was immersed in a solution of 10% HF (at room temperature demonized water dilution). Because the etch rate is much higher in the laser modified region than in the area without laser irradiation, the microchannel can be obtained within 1 h after the etching, as shown in Fig. 1(b) below. Meanwhile, the chemical etching process is performed in an ultrasonic bath in order to facilitate the HF penetrating into the spiral microchannel.

Then, the metal gallium is injected into the manufactured helical microchannel to achieve conductive microcoils. The gallium with purity of 99.99% is used as the metallic conductors. To create the connector for the injection process, a fused-silica sample is placed on a prepared polydimethylsiloxane (PDMS) film, and then two syringe needles are inserted into the PDMS film at the entrance of the channel to connect the whole coils. Thus, the entire channel will be penetrating as integrated. The metal gallium is heated by an alcohol burner before the injection. When the temperature reaches the gallium melting point of 29.8°C, gallium is rapidly liquefied. Liquid gallium is injected at one side of the coil by a syringe pump with a low speed of 0.1 mL/h speed. Meanwhile, it is sucked by a suction pump in another entrance. During injection, the temperature is maintained at about 45°C by infrared heating lamps. When the sample cools down to room temperature, the gallium metal presents full filling of the coil channels, as shown in Fig. 1(c). Then PDMS film is peeled by an ultrasonic bath oscillation after the gallium has solidified completely.

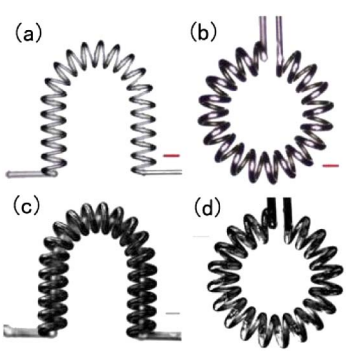

Fig. 2. (a) U-shaped microchannel etched by HF. (b) O-shaped microchannel etched by HF. (c) U-shaped inductance injected with metal gallium. (d) O-shaped inductance injected with metal gallium. The scale bar equals 100 μm.

Nowadays the mainstream microcoil structures are the linear types, which cannot meet the requirements for various applications. Therefore, some complex structures must be used in microelectric systems for satisfying actual purposes. Compared to the linear inductance, U-shaped and O-shaped inductances with special magnetic field distributions can well serve the applications such as biological sample testing, cell filtration, tiny particles trapping, etc.

Figure 2(c) is a U-shaped inductance filled with metal gallium. The length of the straight portion of the channel is about 590 μm. The diameter of the gallium wire is 37 ± 2 μm. The radius of the U-like portion, and the radius and pitch of the coils, are 400, 100, and 68 μm, respectively.

An O-shaped inductance filled with gallium is shown in Fig. 2(d). The radius of the O-shaped circle is 400 μm, and the radius of each of the coils is 100 μm. The diameter of the gallium wire is 36 ± 2 μm. The inductance, L, of the helical microcoils can be estimated by Wheeler's formula:

$$L = \frac{10\pi\mu_0 N^2 r^2}{9r + 10h_{\text{coil}}}. \tag{1}$$

Here, $\mu_0 = 4\pi \times 10^{-7}\ \text{Hm}^{-1}$ is the permeability in free space, N is the number of turns, r is the coil radius, and h_{coil} is the length of the coil. The U-shaped inductance of the liquid-metal coil is calculated to be 3.87 nH. The direct-current resistance of the microcoils is 14.2 Ω. The inductance of the O-shaped liquid-metal coil is calculated to be 9.08 nH. The direct-current resistance of the microcoils is 12.2 Ω.

In the process of fabricating a complex 3D coil, the coil geometry morphology needs to be controlled and adjusted for a wide range of applications: for example, the sensors and actuators need high inductance and a high winding density; the coils for microscale magnetic resonance analysis require high-quality factors and a homogenous magnetic field [12].

The FLWE technology enables flexible and accurate fabrication of the coil with controlled morphology and length. As shown in Fig. 3, we can see that the pitch and the radius of the spiral coil can be adjusted gradually. In Fig. 3(a), the coil pitch changes from 200 μm on the left to 50 μm at the middle, and then expands to the initial 200 μm. In Fig. 3(b), the radius of the coil is gradually

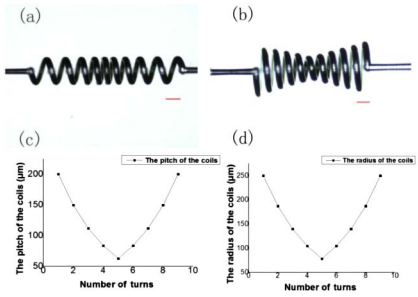

Fig. 3. (a) Pitch-controlled microcoil. (b) Radius-controlled microcoil. (c) Relationship of the turns and the pitch of the coil. (d) Relationship of the turns and the radius of the coil. The scale bar equals 100 μm.

reduced from 250 μm on the left to 80 μm in the middle, and then increases to the initial 250 μm.

In recent research, it is reported that the decrease of the bridging angle in densified silica increases the reactivity of oxygen because of the deformed configuration of the oxygen's valence electrons. This configuration deformation of the femtosecond-laser-irradiated pattern in the silica can be considered in terms of the Lewis base, which is more chemically active in reactions with acids than in materials such as unidentified silica [17]. The microchannels with high uniformity are required for obtaining high-performance microcoils. Therefore, it is key to regulate the reaction of the Lewis base with HF for producing long microchannels with excellent uniformity. We propose an improved FLWE process by introducing extra access ports and power compensation methods.

By creating a series of laser-scanned lines that connect a sample surface with the internal structures, extra access ports are prepared by the chemical process. In that case, HF acid solutions can directly penetrate into the central parts of the channels rapidly. The air in the microchannel was compressed in the extra lines by the liquid Ga, and it will prevent the Ga from being injected into the extra access ports.

Different levels of laser power were used in the laser-scanning process to control the diameters of the microchannels at different sections [18]. To solve the conical-shape problem and to achieve uniformity in the fabricated microchannels, as shown in Fig. 3(b), we investigate the power dependency of the diameters of the chemically etched microchannels as shown in Fig. 4(a). Here, the laser power was changed through tuning a computer-controlled attenuator. To decrease the diameter of the channel near the entrances and access ports, the laser power used in these positions was lower. The laser power was linearly increased to a higher value when the laser focal spot was approaching the middle points of two nearby access ports. The result is shown in Fig. 4(c).

Compared to the linear microcoils, the helical microcoils have relatively complex structures. The longer channel length and more number of turns of the coil make the fluid metal injection a more challenging task. In this case, it is possible to improve the degree of smoothness of the microchannels' inner wall to reduce the flow resistance of liquid metal.

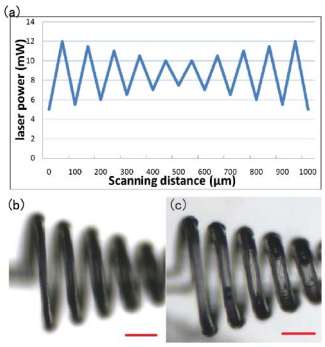

Fig. 4. (a) Laser power curves in the laser writing helical line process. (b) Fabrication without power dependency. (c) Fabrication with power dependency. The scale bar equals 100 μm.

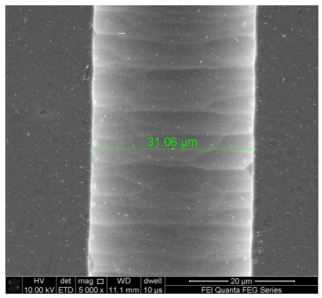

Fig. 5. Morphology of the microchannel observed via an SEM.

Here, four major improvements have been adopted in processing of the complex 3D microcoils, including slower femtosecond laser writing speed, lower laser power, lower HF concentration, and longer etch time. We decreased the concentration of HF, laser power, and scan speed from 10% to 5%, 8 to 6 mW, and 10 to 5 μm/s, respectively. Etching time is about 190 min. In particular, HF etching with lower concentration and longer time has a very apparent effect in improving the channel smoothness. The quality and speed of etching can be controlled by choice of etchant, too [19]. By adopting the abovementioned methods, gallium metal has been successfully injected into the processed microchannels. The microchannel fabricated on the surface of the fused-silica sample after HF treatment can be observed in Fig. 5. It shows a straight microchannel with a scanning electronic microscope (SEM), indicating good uniformity and smoothness of the microchannels.

In summary, by means of improved FLWE technology and metal microsolidifying technology, some complex 3D microcoil structures can be achieved inside fused silica. The microcoils with large aspect ratios are fabricated by the FLWE technology. The microchannels with high uniformity and long channel for high-performance microcoil applications are realized, demonstrating the flexibility and controllability in fabrication of the complex 3D microcoil structures. The proposed technique is promising for fabricating a broad spectrum of microelectric systems based on compact and complex 3D microcoil networks.

This work is supported by the National Natural Science Foundation of China under Grant Nos. 61275008 and 61176113, the Special-funded program on national key scientific instruments and equipment development of China under Grant No. 2012YQ12004706, and the Fundamental Research Funds for the Central Universities.

References

1. S. G. He and F. Chen, J. Micromech. Microeng. **22**, 10 (2012).
2. H. Takahashi, T. Dohi, K. Matsumoto, and I. Shimoyama, in *Proceedings of the IEEE International Conference on Micro Electro Mechanical Systems* (IEEE, 2007).
3. C. H. Ahn and M. G. Allen, J. Micromech. Microeng. **3**, 37 (1993).
4. Y. Lu and H.-F. Ji, Sens. Actuators B **123**, 2 (2007).
5. K. Yoshimura, K. Nakano, T. Miyake, Y. Hishikawa, C. Kuzuya, T. Katsuno, and S. Motojima, Carbon **45**, 1997 (2007).
6. K. Seemann, H. Leiste, and V. Bekker, J. Magn. Magn. Mater. **302**, 321 (2006).

7. C. Massin, G. Boero, F. Vincent, J. Abenhaim, P. A. Besse, and R. S. Popovic, Sens. Actuators A **97–98**, 280 (2002).
8. T. Dohi, K. Kuwana, K. Matsumoto, and I. Shimoyama, in *Proceedings of IEEE Conference on Transducers* (IEEE, 2007).
9. M. J. K. Klein, T. Ono, M. Esashi, and J. G. Korvink, J. Micromech. Microeng. **18**, 075002 (2008).
10. B. Lochel, A. Maciossek, M. Rothe, and W. Windbracke, Sens. Actuators A **54**, 663 (1996).
11. D. A. Seeber, R. L. Cooper, L. Ciobanu, and C. H. Pennington, Rev. Sci. Instrum. **72**, 2171 (2001).
12. K. Kratt, V. Badilita, T. Burger, J. G. Korvink, and U. Wallrabe, J. Micromech. Microeng. **20**, 015021 (2010).
13. S. Goto, T. Matsunaga, Y. Matsuoka, K. Kuroda, M. Esashi, and Y. Haga, in *Proceedings of the IEEE International Conference on Micro Electro Mechanical Systems* (IEEE, 2007).
14. L. O. Sillerud, A. F. McDowell, N. L. Adolphi, R. E. Serda, D. P. Adams, M. J. Vasile, and T. M. Alam, J. Magn. Reson. **181**, 2 (2006).
15. R. Osellame, H. J. W. M. Hoekstra, G. Cerullo, and M. Pollnau, Laser Photon. Rev. **5**, 3 (2011).
16. B.-B. Xu, H. Xia, L.-G. Niu, Y.-L. Zhang, K. Sun, Q.-D. Chen, Y. Xu, Z.-Q. Lv, Z.-H. Li, H. Misawa, and H.-B. Sun, Small **6**, 16 (2010).
17. A. Marcinkevičius and S. Juodkazis, Opt. Lett. **26**, 277 (2001).
18. S. He and F. Chen, Opt. Lett. **37**, 18 (2012).
19. S. Juodkazis and K. Yamasaki, Appl. Phys. A **79**, 4 (2004).